CHAPTER VIII

INHIBITION OF MILD STEEL CORROSION IN IM HYDROCHLORIC ACID USING(E)-4-(2-CHLOROBENZYLIDENEAMINO)-6-METHYL-3-THIOXO-3,4-DIHYDRO-1,2,4-TRIAZIN5(2H) -ONE (CBMTDT)

This chapter is published in Indian Journal of Chemical Technology.

17 (2010) 425-430.

8.1 MEDIUM

The medium for the study was prepared from reagent grade HCl (E Merck) and doubly distilled water. The entire tests are performed in aerated medium under standard conditions.

8.2 INHIBITOR MOLECULE

The inhibitor, CBMTDT was prepared by the procedure described in chapter 3.2. The compound is soluble in 1M HCl at room temperature. The structure of the compound is given in Fig.8.1.

8.3 RESULTS AND DISCUSSION

8.3.1 Weight loss Studies

From the study it is clear that the weight loss enhances with increasing exposure time and decreases with increasing inhibitor concentration. The weight loss data's were used to calculate the corrosion rate using the equation

$$\text{Corrosion Rate} = \frac{534W}{DAt}$$

where W is the loss of weight (mg), D is the density of the specimen, A is the area of the specimen and t is the exposure time in hours. The variations of corrosion rate with exposure time are given in Table Vlll.1. The corrosion rate decreases with increasing concentration of CBMTDT.

8.3.2 Potentiodynamic Polarization Studies

Potentiodynamic polarization studies of mild steel in 1M HCl in the absence and presence of inhibitors were carried out in the potential range from –250 mV to +250 mV with a sweep rate of 1000 mV/ minutes (16mV/sec). The cathodic and anodic polarization curves obtained for mild steel in 1M HCl with various inhibitor concentrations are given in Fig.8.2. The electrochemical parameters like corrosion potential (E_{corr}), cathodic and anodic Tafel slopes (β_c & β_a) and corrosion current density (i_{corr}) obtained from Tafel extrapolation of polarization curve were given in Table Vlll.2. It is clear

from the figure that both the anodic metal dissolution and cathodic hydrogen evolution reactions were inhibited after the addition of CBMTDT to the aggressive medium. The change in the slope of cathodic current–potential line and anodic current–potential line indicates the modification of both anodic and cathodic reaction mechanisms in inhibited solution with time. These results suggest that CBMTDT acts as mixed type corrosion inhibitor [1]. The inhibitor molecules first adsorbed on to the metal surface and impedes by merely blocking the metal sites without affecting the anodic and cathodic reaction mechanism [2]. For the inhibitor, the corrosion current density decreased and inhibition efficiency increased with increasing inhibitor concentration, due to the increase of surface coverage. Linear polarization resistance plot (LPR) is another form of Tafel plot and is depicted in Fig.3. Polarization resistance (Rp) was determined from the slope of the potential versus current lines (LPR plot) and presented in Table Vlll.2. The increase of Rp values with increasing inhibitor concentration is due the adsorption of inhibitor molecule on the metal surface. Thus LPR also agrees the adsorption mechanism of inhibition.

8.3.3 Electrochemical Impedance Spectroscopy

EIS technique provides a rapid and convenient method to evaluate the performance of the organic coating on the metal and has been used for the investigation of protection properties of organic inhibitors. The inhibitor does not disturb the double layer at the metal/solution interface. Therefore, more reliable results can be obtained from this technique. Electrochemical impedance spectroscopy (EIS) measurements were carried out with amplitude of 10mV ac sine wave with a frequency range of 10 KHz to 10Hz with reference to standard calomel electrode (SCE). The Nyquist plot and the representative Bode diagrams for the mild steel after 1 hour exposure in uninhibited and inhibited 1M HCl are given in Fig.8.4 & 8.5**.** The semicircular appearance of the impedance diagram shows that a charge transfer process mainly controls the corrosion of mild steel [3]. Polarization resistance which corresponds to the diameter of Nyquist plot includes charge transfer resistance (R_{ct}), diffuse layer resistance (R_d), accumulation resistance

(Ra), film resistance (R_f), etc. The charge transfer resistance which determines the corrosion rate corresponding to the resistance between the metal and Outer Helmholtz Plane (OHP) [4-5].Table Vlll.4 lists the important parameters obtained from impedance spectra**.** R_{ct} and C_{dl} values have opposite trend through out the analysis. The decrease in electrical double layer capacitance with increase in inhibitor concentration may be attributed to the formation of a protective layer on the electrode surface and thus reduces corrosion rate. The adsorbed layer of the inhibitor molecule displaces the water molecule and other ions originally adsorbed on the metal surface [6].The values of corrosion inhibition efficiency (%IE) is also given in the Table Vlll. 3. The results obtained from the electrochemical measurements support the data derived from weight loss measurements.

8.3.4 Adsorption Studies

The adsorption isotherm can provide basic information on the interaction of inhibitor with metal surface [7-8].To obtain adsorption isotherm, the surface coverage values (θ) for different concentrations of inhibitor in 1M HCl have been obtained from potentiodynamic polarization measurements. Using these data different graphs has been constructed to find out the most suitable adsorption isotherm. The plot log (θ/1-θ)Vs log C yields a straight line with a slope of 1.4416 & R^2=0.9139, indicating that the adsorption of the CBMTDT on mild steel surface obey Langmuir adsorption isotherm and is shown in Fig.8.6.

8.3.5 Quantum Chemical Calculations

To study the effect of molecular structure on the inhibition efficiency of the CBMTDT, ab initio quantum chemical calculations were performed using density functional theory (DFT).The charge distribution on the inhibitor molecule ranges from -0.616 to 0.616. Some quantum chemical values were computed using DFT and energies of highest occupied molecular orbital (E_{HOMO}=-1.8231eV), lowest unoccupied molecular orbital (E_{LUMO}=-5.7555 eV) and total energy (E_{total} = 795676.40 kcal/ mol) are also calculated .The dipole moment of the molecule is calculated to be 4.0852 D. The inhibition

efficiency of a molecule related to the metal-orbital interactions. Good inhibitor molecules offer electrons to the unoccupied orbital of metal and accept free electrons from the metal. That is a charge transfer phenomenon may takes place between the metal and the inhibitor molecule, which confirms that adsorption of the inhibitor is the basis for inhibitory action towards mild steel in 1M HCl. From quantum chemical calculations, it is clear that higher the HOMO energy of the inhibitor, greater is the trend of donating electrons to the unoccupied 'd ' orbital of the metal, and higher the corrosion inhibition efficiency. The lower LUMO energy level makes easy acceptance of electrons from the metal surface. The magnitude of ΔE value ($\Delta E = E_{LUMO} - E_{HOMO}$) also help us to predict probable roots of the inhibitory action [9-10]. Smaller the ΔE value greater is the inhibitory action. Here the lower value of ΔE also agrees the excellent inhibition efficiency of CBMTDT towards mild steel in 1M HCl solution.

8.3.6. Local Selectivity

The local reactivity of CBMTDT is analyzed by means of the condensed Fukui function. The condensed Fukui functions and condensed local softness indices allow us to distinguish each part of the molecule on the basis of its distinct chemical behavior due to the different substituent functional groups [11]. Thus, the site for nucleophilic attack will be the place where the value of $\int^{+}$ is the maximum. In turn, the sight for electrophilic attack is controlled by the value of $\int^{-}$, for nucleophilic attack the most reactive site of CBMTDT is on the C (14) atom. For electrophilic attack the most reactive site of CBMTDT is on the S (23) atom. It is clear that C (14) has more nucleophilic character and is involved in the chemical reactivity of the molecule with metal surface, which explains the adsorption mechanism of inhibitor on mild steel surface in hydrochloric acid. The optimized geometry of CBMTDT is given in Fig.8.7 and the results are given in Table lll.4B of chapter lll. The condensed local softness indices Sk^{-} and Sk^{+} are related to the condensed Fukui functions. The local softness follows the same trend of Fukui functions.

8.4 CONCLUSION

- The compound, CBMTDT in 1M HCl possess excellent inhibition efficiency for mild steel corrosion.

- As the concentration of the inhibitor increases, corrosion inhibition efficiency and charge transfer resistance increases whereas the corrosion rate and double layer capacitance decreases due to more adsorption of the inhibitor.

- The inhibitor molecule affects both the anodic and cathodic processes and hence acts as a mixed type inhibitor.

- The adsorption of the inhibitor obeys Langmuir adsorption isotherm model.

- Quantum chemical calculations show that, the increase in the energy of the HOMO of the inhibitor molecule promotes its tendency of electron donation to the unoccupied 'd' orbital of the metal and the lowering of the energy of the LUMO tend to increase its electron accepting power and the combined effect also increases the corrosion inhibition efficiency.

8.5 REFERENCES

1 . Fuchs-Godec.R, *Colloids Surf.A:Physicochem.Eng.Aspects*.280 (2006) 130.

2. Abdel-Rehim.S.S,Ibrahim.M.A.M & Khaled.K.F,*Mater.Chem.Phys*.70 (2001) 268.

3. Hui-Long Wang, Rui-Bin Liu & Jian Xin, *Corros. Sci.* 46 (2004) 2455.

4 . Erbil.M, *Chim.Acta Turcica*. 1 (1988) 59.

5 . Solmaz.R,Kardas.G,Yazici.B & Erbil.M, *Colloids and Surfaces A*. 312 (2008).

6 . Lebrini.M, Lagrenee.M, Vezin.H ,Gengembre.L & Bentiss.F, *Corros. Sci.* 47 (2005) 485.

7 . Migahed.M.A,Monhamed.H.M & Al-Sabagh, *Mater.Chem.Phys*.80 (2003) 169.

8. Azim.A, Shalaby.L.A & Abbas.H, *Corros Sci*. 14 (1974) 21.

9 . Lukovits.I, Palfi.K & Kalman.E , *Corros Sci*. 53 (1997) 915.

10 . Ozcan & DehriI, *Prog Org Coat*. 51(2004) 181.

11 . Fukui.K,Yonezawa .T & Shingu .H, *J Chem. Phys*.20 (1952) 722.

Table Vlll.1 Corrosion rate of mild steel in 1M HCl solution in the presence of various concentrations of CBMTDT.

Conc: in(ppm)	Corrosion rate (mpy) with time in Hours			
	24	48	72	96
0	12875	8881	6148	4741
10	11537	7111	4927	3874
25	1724	1090	892	743
50	1559	972	710	606
75	1445	870	674	542
100	952	751	582	478
200	851	621	473	387

Table Vlll.2 Electrochemical parameters for mild steel obtained from polarisation curves in 1M HCl at 300K.

Conc (ppm)	E_{corr} (mV)	R_p (Ω/cm^2)	β_a (mV/dec)	β_c (mV/dec)	i_{corr} ($\mu A/cm^2$)	IE %	C.R (mpy)	Surface coverage (Θ)
0	-484	8	121	144	3601	---	601	----
10	-501	11	101	139	1841	50	360	0.4009
25	-515	13	75	102	1622	55	239	0.6023
50	-509	16	80	121	1443	61	140	0.7670
75	-510	19	109	167	1304	63	99	0.8352
100	-500	40	66	113	443	87	27	0.9550
200	-504	35	67	66	412	89	13	0.9783

Table Vll.3 AC impedance data of mild steel with CBMTDT at 300K in 1M HCl.

Conc (ppm)	R_{ct} (Ω cm^2)	C_{dl} (μF cm^{-2})	i_{corr} ($\mu A/cm^2$)	IE %	C.R (mpy)
0	23	220	1120	----	512
10	31	130	817	27	373
25	69	111	377	66	172
50	100	102	259	77	118
75	132	106	197	82	90
100	300	99	86	92	39
200	579	31	45	96	20

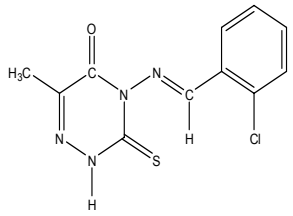

Fig .8.1 Structure of the inhibitor molecule.

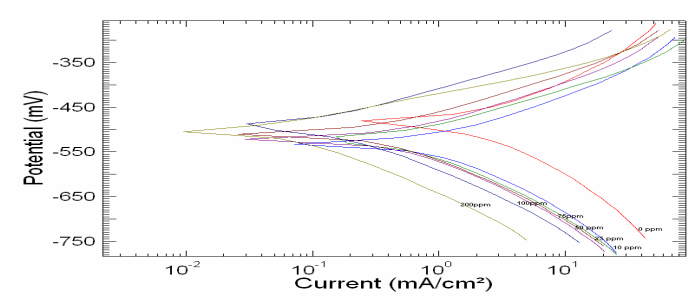

Fig.8.2 Potentiodynamic polarization curve for mild steel in1M HCl in the absence and presence of different concentration of CBMTDT at 300 K.

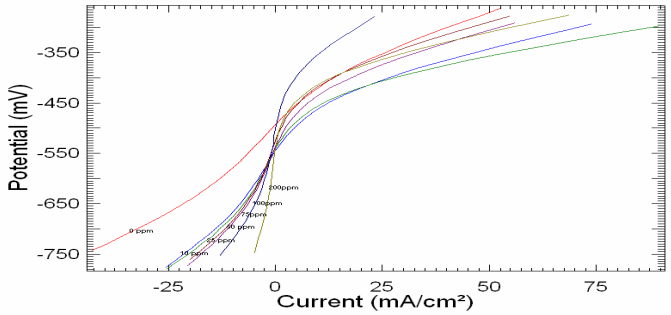

Fig .8.3Linear polarization curves for mild steel in 1M HCl in the absence and presence of different concentrations of CBMTDT at 300 K.

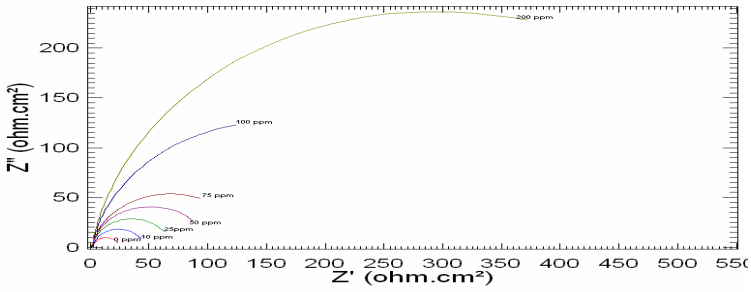

Fig.8.4Nyquist plots for mild steel in 1M HCl in the absence and presence of different concentrations of CBMTDT at 300 K.

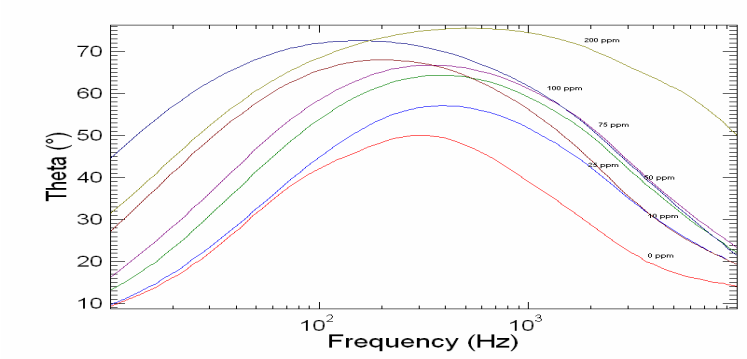

Fig.8.5Bode curves for mild steel in 1M HCl in the presence of different concentrations of CBMTDT at 300 K.

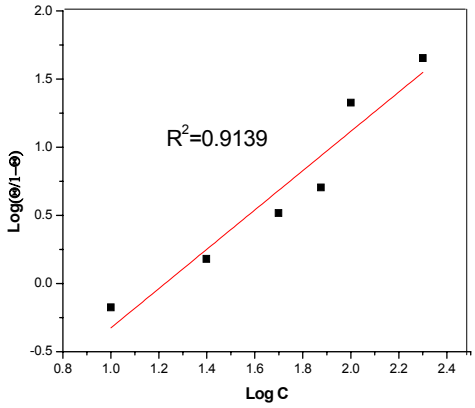

Fig.8.6 Langmuir adsorption isotherm for mild steel in 1M HCl at 300 K in the presence of CBMTDT.

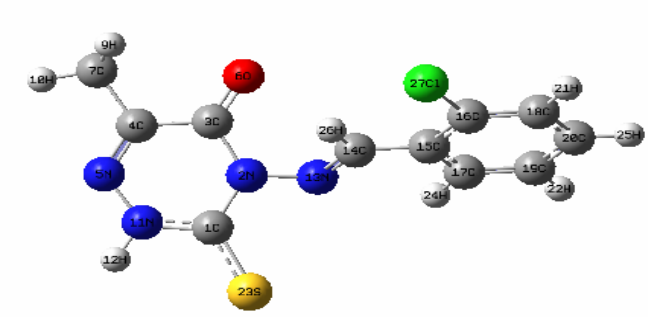

Fig.8.7 Optimized geometry of the CBMTDT molecule.